ACS OMEGA

Open Access

http://pubs.acs.org/journal/acsodf

Article

Synthesis Method and High Salt Concentration Can Affect Electrodeformation of GUVs under Strong Pulsed DC Fields

Mohammad Maoyafikuddin, Shrikrishna V Kulkarni, and Rochish M. Thaokar*

Cite This: *ACS Omega* 2025, 10, 6427−6436

Read Online

ACCESS | Metrics & More | Article Recommendations

ABSTRACT: The study focuses on two important issues in the electrodeformation of giant unilamellar vesicles (GUVs) as biomimic objects, with regard to their electroporation. The results are presented with respect to the ratio of the conductivities of the inner and outer fluids of the GUV, ($\beta = \Lambda_{en}/\Lambda_{sus}$), and the concentration of salt in the enclosed medium (C_{en}). In this work, low and high salt concentration regimes are referred to as $C_{en} \leq 0.3$ mM and $C_{en} \geq 25$ mM respectively. First, responses of GUVs under strong pulsed DC fields are observed to be sensitive to the synthesis methods (electroporation or gel-assisted method) for both $\beta = 1$ and $\beta < 1$ in the low salt concentration regime. This might be caused by a higher initial membrane tension (in the case of electroformed GUVs) or possibly a greater membrane edge tension (in the case of GUVs prepared by the gel-assisted method). Second, the effect of salt concentration on the electrohydrodynamic behavior of GUVs under strong pulsed DC fields indicates that the extent of poration and pore growth and, correspondingly, the shape deformation can be qualitatively different at different salt concentrations. This suggests the possibility of higher edge tension in GUVs as well as faster "electrical shorting" of the membrane due to the abundance of ions and thereby lower pore growth in high-salt GUVs. The study shows that the extrapolation of results obtained in GUV electroporation to biological cells should be done with caution.

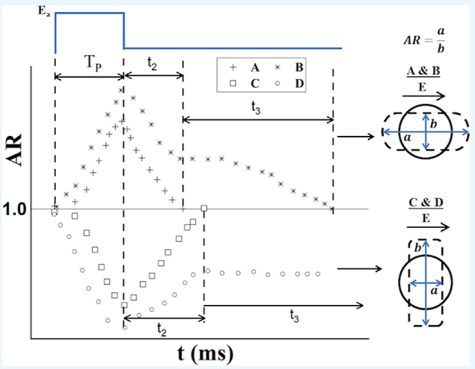

INTRODUCTION

Electroporation of biological cells is a complex process, predominantly due to the irregular shape of cells, and highly structured biological membranes, which have complex constitutions made up of multicomponent lipids, membrane proteins, cholesterols, etc, due to the presence of complex intra and extracellular structures such as actin and myosin, cytoskeleton, glycocalyx and spectrin and many internal cell organelles.[1] This renders elucidating the physics of electroporation of biological cells and cell membranes extremely difficult. To overcome such difficulties, Giant Unilamellar Vesicles (GUVs), made up of a single lipid bilayer and of size, bigger than 5−10 μm, and widely considered to be the best biomimic objects for biological cells, have been extensively studied for systematic investigations of their response under electric fields.[2]

When a GUV is subjected to a strong DC pulsed electric field for a sufficiently long time, a transmembrane potential, $V_v = 3/2E_aR_v\cos\theta$ is induced in the membrane where E_a, R_v and θ denote the peak value of the applied electric field, the radius of the vesicle, and polar angle measured with respect to the direction of the electric field, respectively. When the electrical energy, W_E (see eq 1) associated with the transmembrane potential overcomes the net energy barrier, W_{edge} (see eq 2) associated with the interplay of edge tension of the membrane and the membrane tension, hydrophilic pores of the radius of r_{pore} form in the membrane,[3,4] and the process is termed as electroporation. Here, ϵ_0, ϵ_{med}, ϵ_L, d_L, and γ_L represent absolute permittivity, dielectric constants of the enclosed and suspending mediums, dielectric constants of the lipid bilayer membranes, thicknesses of the lipid bilayer membranes, and edge tension of the membrane, respectively.

$$W_E = \frac{1}{2}\epsilon_0 \frac{\epsilon_{med} - \epsilon_L}{d_L} V_v^2(\pi r_{pore}^2) \quad (1)$$

$$W_{edge} = \gamma_L(2\pi r_{pore}) - \sigma(\pi r_{pore}^2) \quad (2)$$

The relevance of studying the electroporation of vesicles (GUVs) is 2-fold. While it greatly helps elucidate the mechanism of electroporation in cellular membranes, which is otherwise complex, it also helps in making advances toward establishing GUVs as biomimetic objects for biological cells. GUVs are being increasingly manipulated to construct reconstituted biological cells, with controlled membrane

Received: July 11, 2024
Revised: December 5, 2024
Accepted: December 25, 2024
Published: February 14, 2025

composition, internal organelles,[5] and actin network[6] etc, that are introduced inside the GUVs, step by step in the laboratory, using various methods. In this pursuit, understanding the electroporation of GUVs will eventually help us understand the electroporation of reconstituted biological cells.

Vesicles in strong electroporating fields undergo ellipsoidal shape deformations in the absence of ions, which can be temporally visualized in high-speed microscopy with a resolution of around tens of thousands of frames per second.[7] Riske and Dimova[8] investigated the role of ions (∼1 mM NaCl) in vesicle deformation using a single DC electric pulse and observed the flattening of the vesicles, which was attributed to the electrophoretic force of the ions. In their work, the resulting shapes, referred to as cylindrical deformations, are characterized as disc (for $\beta < 1$), square ($\beta = 1$), and tube ($\beta > 1$) shapes. Here, $\beta\left(=\frac{\Lambda_{en}}{\Lambda_{sus}}\right)$ represents the conductivity ratio, and Λ_{en} and Λ_{sus} are the conductivities of the enclosed and the suspending medium respectively. Our recent research demonstrated that the cylindrical deformations are not specific to unipolar DC pulse but also to other waveforms (bipolar and sinusoidal pulses) and are observed even in the absence of added ions (as an electrolyte).[9] We conjectured that the transmembrane potential and possible electroporation play a critical role in such shape deformations, as well as their relaxation on cessation of the applied field.

Several other studies have reported on GUV deformation under pulsed DC fields. Salipante and Vlahovska[10] reported the occurrence of morphological changes in vesicles using a two-pulse technique. This method involved the application of a strong and short pulse (4 kV/cm, 20 μs), followed by a weaker and longer pulse (0.2 kV/cm, 50 ms). The motivation to use two-pulse stimulation in their work was to limit electroporation such that prolate shapes are recovered at the end of the second pulse. The response of GUVs to strong DC pulses is further complicated by lipid loss, shrinkage, as well as an increase in excess area in other cases, in addition to vesicle deformation.[11,12] Readers are encouraged to refer to a comprehensive review by Dimova et al.[13] and Perrier et al.[14] for further understanding of this matter.

Thus, the high deformation observed in GUVs under electroporating pulsed DC fields complicates the process of electroporation. The poration of a GUV, (or for that instance a biological cell), can significantly change membrane conductance, thereby the electric field distribution and associated Maxwells stress, and affect the shape deformation. On the other hand, the shape deformation can alter the electric field distribution and thereby affect the transmembrane potential and the susceptibility to electroporation. Thus a two-way coupling is expected between deformation and poration.

It is important to ask the question, is such high electrodeformation as seen in GUVs observed even in biological cells? Cellular deformation under porating electric fields is complicated by the initial nonspherical shape of the cell and the complex rheology of both the internal cytoplasm as well as the cellular membrane. The high deformation GUV response to strong pulsed DC fields thus seems to contradict the observations in biological cells. It should be noted that the deformation of GUVs subjected to a DC pulsed electric field has been extensively investigated under low salt conditions, $C_{en} \sim 1$ mM where C_{en} is the concentration of ions in the enclosed medium. On the contrary, the physiological salt concentration in biological cells is typically around $C_{en} \sim 150$ mM.[15] Thus, understanding the responses of GUVs prepared in high salt ($C_{en} \geq 25$ mM) concentration would be biologically relevant. The deformation of vesicles in the presence of high salt is expected to be different due to the sensitivity of edge tension to the ionic concentration as supported by molecular dynamics simulations as well as experimental studies[16,17] as well sensitivity of the number of pores and the size of pores to the relative time scales of charging time of the membrane (that depends on the salt concentration) and the pulse width. Moreover, the pore dynamics, when the inner and outer fluids of the vesicle are of different conductivities are reported to be complex due to different ionic (∼1 mM NaCl) activities on either side of the pore.[18] Thus to render the studies on GUVs under pulsed electric fields relevant to cellular electroporation, it is important to investigate the electrodeformation of GUVs with physiologically relevant salt concentration, an issue poorly addressed in the literature.

In most reported studies,[6−10] giant vesicles used for electrodeformation studies, were prepared by the electroformation method. This employs an electric field to swell a dried lipid film in an aqueous solution[19] and produces mostly tensed vesicles (indicating high tension in their membrane) which could be attributed to the oxidation of lipids due to the electric field.[20−22] On the other hand, in the gel-assisted method, the inherent swelling of hydrophilic gel materials causes swelling of lipids and, subsequently, the formation of GUVs,[23,24] and it does not employ any electric field. Hence, vesicles prepared by these two methods might be different as indicated by the sensitivity of the electromechanical properties of vesicles to the synthesis methods Faizi et al.[25] Thus, understanding the differences and similarities of electroporation aspects of GUVs prepared by the electroformation and gel-assisted methods, the two most commonly used methods of making GUVs, is critical, since conflicting data could come from experimental laboratories using GUVs synthesized by one method or the other. The work presented here addresses this very important issue.

In this work, the effect of a DC pulsed electric field on vesicles prepared in low salt (≤0.3 mM NaCl) concentration using the electroformation and gel-assisted method is first examined. Thereafter, the results on GUVs prepared in the presence of high salt (≥25 mM NaCl) concentrations, using the gel-assisted method, and subjected to a pulsed DC electric field are presented.

EXPERIMENTAL SECTION

Materials. High-purity solvents (chloroform and methanol) and other chemical reagents (sodium chloride, sucrose, and glucose) were obtained from Merck, India. Synthetic lipid (Make: Avanti Polar Lipids, 1-stearoyl-2-oleoyl-sn-glycero-3-phosphocholine [SOPC]) was procured from Sigma-Aldrich. All of the chemicals were used without further purification.

Synthesis of Giant Vesicles. Giant vesicles were prepared by two methods, the electroformation method (EF)[26] and the gel-assisted method (GA).[27] In the electroformation method, a pair of conducting (indium tin oxide) glass slides were coated with the SOPC lipid dissolved in a mixture of chloroform and methanol (2:1) using the spin coating technique and was dried in a vacuum for sufficient time to evaporate the organic solvent. Then the electrodes were arranged as a sandwich by using a silicone spacer (thickness ∼3 mm). An aqueous solution of 0.1 M sucrose was injected into the chamber, and an electrical voltage (5 V_{pp}, 10 Hz) was applied across the

https://doi.org/10.1021/acsomega.4c06412
ACS Omega 2025, 10, 6427−6436

electrodes for 4 h. The surface-attached vesicles were pipetted out by a syringe and suspended in a 0.1 M glucose solution to which either salt was added or not added, depending upon the requirements of the electrodeformation experiment.

The gel-assisted method was mostly used to prepare vesicles in an aqueous medium containing 0.1 M sucrose and an appropriate amount of salt, and starch was used as the gel material. Using literature protocols, a 2 wt % gel was prepared and lipid solution was coated on the gel surface and dried in a vacuum to remove the organic solvent.[27] The lipid layer coated on the gel surface was hydrated for half an hour. Finally, the solution containing GUVs was sucked out and mixed with 0.1 M glucose solution, either containing or not containing added salt. To realize $\beta\left(=\frac{\Lambda_{en}}{\Lambda_{sus}}\right) \leq 1$, no salt or an appropriate amount of salt was added to the suspending medium of the vesicles. Conversely, to obtain $\beta > 1$, vesicles were first synthesized in the presence of salt and then diluted. The concentration of salts for different vesicular samples is depicted in Table 1, where C_{en} and C_{sus} are concentrations of salt in the enclosed and suspending medium of vesicles respectively.

Table 1. Concentrations of Ions in the Enclosed and Suspending Medium of Vesicles

samples	C_{en} (mM)	C_{sus} (mM)	$\Delta C = C_{en} - C_{sus}$ (mM)
EF-A & GA-A	0	0	0
EF-B & GA-B	0	0.476	−0.476
GA-C	25	25	0
GA-D	50	50	0
GA-E	0.3	0.15	0.15
GA-F	100	50	50
GA-G	0.3	0.62	−0.32
GA-H	25	59.52	−34.52

Vesicles prepared using the electroformation and gel-assisted method were suspended in an aqueous glucose solution with or without salt and kept standing for 30 min. It is to be noted that the addition of glucose to the suspending medium helps vesicles to settle down at the bottom, thereby providing better visualization in optical microscopy. The vesicles were assumed to reach an equilibrium state and shape by the end of the settling period of 30 min. The addition of salt to the suspending medium is known to cause deflation of vesicles, leading to morphological change of vesicles. On the contrary, dilution of the suspending medium might cause inflation of vesicles leading to rupture of vesicles. In the present work, vesicles were not continuously monitored for shape changes during this settling period. It is noteworthy that after the vesicles had settled, only well-formed spherical vesicles were considered for electrodeformation experiments. These vesicles did not show reduced volume due to deflation. The conductivity in the enclosed and suspending medium of the vesicle could not be independently determined at the end of the settling period and during the intervals between the incremental application of the electric field.

Electrodeformation Experiments. In any typical experiment, a BTX electroporator (Model ECM830) was used to apply a monopolar, positive DC pulse to a GUV solution, held in an Eppendorf microfusion chamber and having an interelectrode spacing of 0.5 mm. The experiments were carried out under an inverted microscope (Make: Nikon, Model TE2000U) equipped with a differential interference contrast (DIC) enabled objective (Magnification: 40×) and a high-speed camera (Make: Vision Research, Model: Miro-Ex4). To enable recording images at 8000 fps, a high-power halogen lamp (250 W and luminescence of 10,000 lm) was used instead of the commonly used low-power halogen lamp (100 W).

In this study, the vesicles were subjected to a single pulse ($N = 1$), a DC pulsed waveform with an electric field of varied strength (E_a = 0.5−2 kV/cm), and pulse width T_P = 1 ms and the shape deformation and degree of deformation of the GUVs were studied as a function of E_a and β. Here, the degree of deformation of vesicles was characterized by their aspect ratio (AR = a/b), which is the ratio of their length (a) along the direction of the electric field to their length (b) perpendicular to the electric field. A vesicle was randomly selected in any typical experiment, a DC pulsed electric field was applied, and deformation was recorded. The same vesicle was subjected to a successively increased electric field, and an idle time (∼10 min) was maintained between two successive pulses for complete recovery of the vesicle under investigation. At any specific experimental condition, at least six vesicles were considered for the analysis of vesicle deformation to account for the varied behavior of the vesicles and the inherent scatter in the experiments. Thus, any set of microscopy images depicts the shape deformation of the same vesicle as a function of E_a for a given experimental condition unless otherwise stated. Only in one set of experiments vesicles GA-H were directly subjected to 2 kV/cm instead of incremental field.

The electrohydrodynamic behavior of vesicles is characterized by three time scales, the time taken for the membrane to charge referred to as the membrane charging time, T_L (see eq 3),[28]

$$T_L = \frac{R_v C_L}{\Lambda_{en}}\left(1 + \frac{\beta}{2}\right) \tag{3}$$

the time required for charge accumulation at the membrane interface, a phenomenon known as Maxwell−Wagner polarization, characterized by the time scale T_{MW} (see eq 4)[29]

$$T_{MW} = \frac{3\epsilon_0\epsilon_{med}}{\Lambda_{en} + 2\Lambda_{sus}} \tag{4}$$

and the deformation time scale, associated with the Maxwell stresses (see eq 5).[30]

$$T_{EH} = \frac{\eta_{sus}}{\epsilon_0\epsilon_{med}E_a^2} \tag{5}$$

Here, $\epsilon_0 = 8.854 \times 10^{-12}$, $\epsilon_{med} \sim 80$, $\epsilon_L \sim 2.2$, $d_L \sim 5$ nm,[31] $C_L(\sim\epsilon_0\epsilon_L/d_L \sim 0.4\ \mu F/cm^2)$ is the capacitance of the lipid bilayer membrane,[30,32,33] $\eta_{sus}(\sim 10^{-3}$ Pa s) is the viscosity of the suspending medium. If T_P is greater than T_L, then vesicles are assumed to be fully charged at the end of the pulse. On the other hand, T_P being greater than T_{MW} implies that the accumulation of charge occurs at the interface within the time of T_P. Moreover, vesicles are said to be deformable within the time equal to T_P if they successfully overcome the viscous drag force of the surrounding, that is, $T_P > T_{EH}$.

Upon withdrawal of the applied electric field, the vesicles can relax over three different timescales, t_1, t_2, and $t_2 + t_3$. Unporated and spherical-shaped vesicles relax over the time scale of t_1 (refer to eq 6) due to the viscosity (η_L) of the membrane where the membrane tension can be considered to be of the order of the lysis tension (σ_L) of the membrane.[7]

https://doi.org/10.1021/acsomega.4c06412
ACS Omega 2025, 10, 6427−6436

Table 2. Experimental Conditions and Compositions of Vesicular Solutions Used for Electrodeformation Experiments where the Prefix GA and EF Stand for the Gel-Assisted Technique and Electroformation Method, Respectively, Transmembrane Potential (V_v) of Vesicles of Radius 10−20 μm are 0.75−1.5 V, 1.5−3 V, 2.25−4.5 V, and 3.0−6.0 V for E_a = 0.5, 1, 1.5, 2.0 kV/cm, Respectively, and T_{EH} is Determined to Be in the Range of 0.04−0.56 ms for E_a = 0.5−2 kV/cm

GUV	C_{en} (mM)	Λ_{en} (μS/cm)	Λ_{sus} (μS/cm)	β	T_L	T_{MW}
EF-A						
GA-A	0	1.43	1.48	1	0.4−0.8 ms	4.8 μs
EF-B						
GA-B	0	1.43	56	0.03	0.28−0.55 ms	0.18 μs

$$t_1 = \frac{\eta_L}{\sigma_L} \tag{6}$$

Relaxation of porated vesicles is assisted by the closure of pores over t_2 (refer to eq 7) when the gain of the excess area (ΔA) of vesicles due to poration is small.[7]

$$t_2 = \frac{\eta_L r_{pore}}{2\gamma_L} \tag{7}$$

For vesicles, in which, ΔA is significant after the application of the electric field, the relaxation follows both t_2 and t_3 mechanisms, implying that the vesicles lose internal volume due to water efflux, leading to much greater excess area, and the shape relaxes over time scale t_3 (refer to eq 8).[34] Here, K_L(=10^{-19} J) is the bending elasticity of the membrane[35−39]

$$t_3 = \frac{4\pi R_v^3 \eta_{sus}}{3K_L}\left(\left(1 + \frac{\Delta A}{4\pi}\right)^{3/2} - 1\right) \tag{8}$$

The typical values of t_1 and t_2 of vesicles are expected to be of the order of 100 μs (where $\sigma_L \sim 5$ mN/m[32] and $\eta_L \sim 3.5 \times 10^{-7}$ N s/m[40]) and 10 ms (for r_{pore} = 1 μm) respectively. Given that the critical transmembrane potential for the vesicles is approximately 1 V,[41] vesicles exhibiting a transmembrane potential exceeding 1 V can be considered to have relaxed over the timescales of either t_2 or $t_2 + t_3$. Since the determination of the location of pores in the membrane was visually difficult, the representative sizes of the pores, in this work, were determined from t_2 using eq 7.

RESULTS AND DISCUSSION

Effect of GUV Preparation Method on the Low Salt Limit. To investigate whether synthesis protocols affect the electrodeformation behavior of vesicles in a DC-pulsed electric field, vesicles prepared by both the EF and GA methods were subjected to a successively increasing electric field in the range of 0.5−2 kV/cm, in the incremental fashion, and their degree of deformation and relaxation characteristics are compared and analyzed. The conductivities of the vesicular systems used in these experiments are shown in Table 2. Experiments were conducted for β = 1 and β < 1. The yield of vesicles of desired sizes (≥10 μm) was very poor when vesicles were prepared in a low ionic (~0.3 mM NaCl) environment using the standard electroformation method. Therefore, experiments for comparison of the response of electroformed and gel-assisted GUVs to pulsed DC fields could not be carried out for β > 1.

For β = 1, and with no added salt in both the regions, it is observed that at the low electric field, i.e., E_a = 0.5 kV/cm, the degree of deformation of vesicles EF-A and GA-A is comparable. On the other hand, the deformation of vesicles EF-A is greater than that of GA-A at a higher electric field, i.e., E_a = 2 kV/cm (refer to Figure 1).

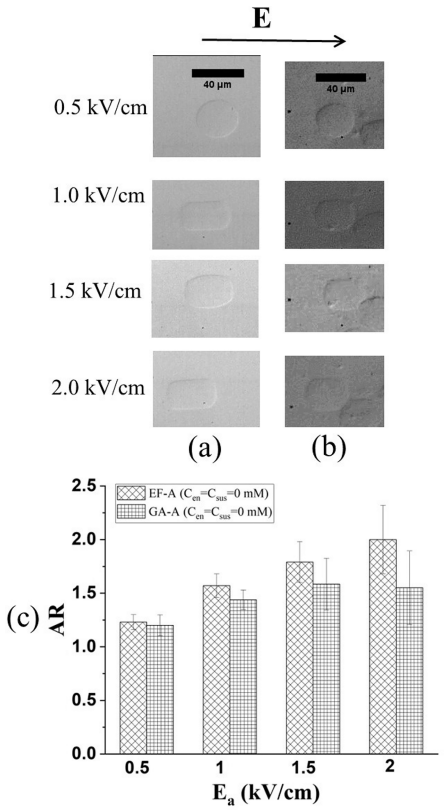

Figure 1. Microscopy images of shape deformations of vesicle (a) EF-A and (b) GA-A at t = 1 ms for E_a = 0.5−2 kV/cm, and (c) comparison of AR of vesicles at t = 1 ms.

When the suspending medium has higher conductivity than the enclosed medium (β < 1), at a low electric field (E_a = 0.5 kV/cm), vesicles EF-B exhibit prolate ellipsoidal deformation (refer to Figure 2a) as indicated by the value of AR (1.13 ± 0.05) at t = 1 ms. This is contrary to the observation in the literature that vesicles exhibit oblate deformation for β < 1 (Figure 2a).[8] This is really due to the complete charging of the vesicles at the end of 1 ms, where, in the absence of poration, GUVs are known to acquire prolate or spherical shapes due to compressive stresses at the equator. This is supported also by the data for the vesicle at 0.5 kV/cm.[42] As the electric field is increased to 1.0 kV/cm, oblate cylindrical (AR = 0.62 ± 0.1 at t = 1 ms) deformation is observed, indicating increased and significant charge accumulation at the interface, accompanied by poration of the membrane. A further increase in the electric field to 1.5 kV/cm leads to a stronger electrohydrodynamic force causing asymmetric disruption at the two poles of the vesicle and thereby leading to an irregular shape for which AR can not be faithfully calculated. This is also seen clearly in the time-lapse images presented for the case of 1.5 kV/cm in

https://doi.org/10.1021/acsomega.4c06412
ACS Omega 2025, 10, 6427−6436

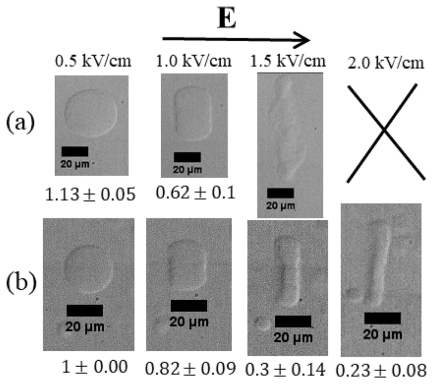

Figure 2. Microscopy images of shape deformations of vesicles (a) EF-B and (b) GA-B at t = 1 ms for E_a = 0.5−2 kV/cm, the numerical figures beneath each image indicate the AR of vesicles at t = 1 ms.

Figure 3a. The experiment can not be continued for E_a = 2.0 kV/cm due to the nonrecovery and dislocation of the EF-B vesicle.

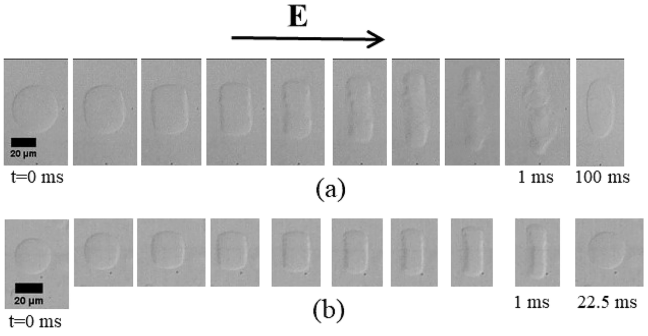

Figure 3. Time-lapse images of vesicles (a) EF-B and (b) GA-B exposed to a DC pulsed electric field of E_a = 1.5 kV/cm.

The above experiments are then carried out with vesicles GA-B for E_a = 0.5−2 kV/cm. Figure 2b depicts the shape deformation of these vesicles at E_a = 0.5 kV/cm, in which no visible deformation of the vesicle is observed at the end of the pulse (1 ms), indicating complete charging of the unporated vesicle. However, vesicles deform into oblate cylinders due to compressive maxwell stress generated at the pole of the vesicles as the electric field is increased to and beyond 1.0 kV/cm. Similar to the β = 1 case, the deformation in the gel-assisted vesicles is distinctly lower than that of the electroformed vesicles (Figure 2b) (AR = 0.62 ± 0.1 vs AR = 0.82 ± 0.09 for EF-B and GA-B respectively at E_a = 1.0 kV/cm). At 1.5 kV/cm, vesicles GA-B continue to show systematic oblate deformation, unlike vesicles EF-B in the same field. although admitting significantly higher deformation, and thereby poration (See Figures 3b and 2b and Table 3). Even at a significantly higher field of 2.0 kV/cm, the vesicles GA-B show fairly well-controlled electroporation (Figure 2b).

The relaxation characteristics of vesicles prepared by the electroformation method and the gel-assisted technique are further compared and are summarized in Table 3. For β = 1, vesicles EF-A and GA-A are observed to relax in 14.4 ± 3.6 and 9.8 ± 3.6 ms respectively predominantly following the t_2 mechanism where probabilities of occurrence of t_3 mechanism, $P(t_3)$ are around 16 and 9% for vesicles EF-A and GA-A respectively. For β < 1, the relaxation characteristics of vesicles prepared by the electroformation method and the gel-assisted method are compared in Figure 4. In the case of vesicles EF-B

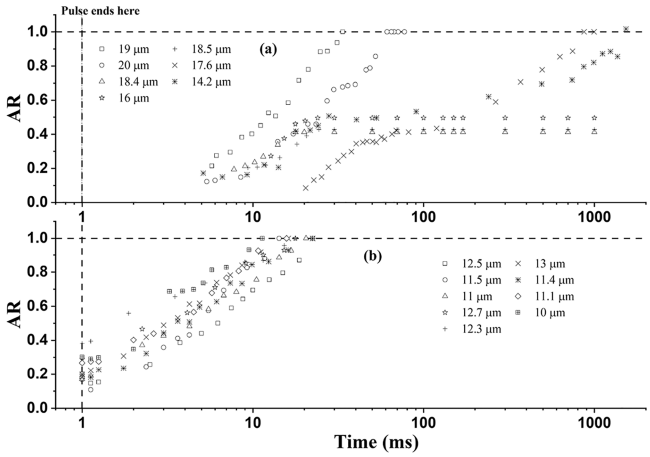

Figure 4. Relaxations of vesicles (a) EF-B and (b) GA-B where E_a = 1.5 kV/cm.

(refer to Figure 4a), AR can not be measured until the vesicle adopts a regular shape. In fact, a great fraction of vesicles ($P(t_3) \sim 70\%$) relax following the t_2 and t_3 mechanism in the case of electroformed vesicles. On the other hand, all the vesicles prepared by the gel-assisted method, that is, GA-B relax over 17.6 ± 3.7 ms (refer to Figure 4b) following the t_2 mechanism. The above discussion shows that the relaxation characteristics of vesicles are sensitive to the synthesis method when the conductivity of the suspending medium is kept greater than that of the enclosed medium.

The difference in the electrohydrodynamic response of EF and GA vesicles can be attributed to the different edge tensions and/or the initial tension in the vesicles made by the two methods. Higher membrane tension can admit greater poration and thereby slower relaxation. Higher edge tension, on the other hand, would mean lower electroporation and faster closure. It appears that at higher electric fields, the electroformed vesicles show larger deformation regardless of the conductivity ratio, β. Even though vesicles synthesized by both methods show similar relaxation behavior for β = 1, their relaxation characteristics are different for β < 1. This suggests

Table 3. Comparison of Relaxations of Vesicles Prepared by the Electroformation Method and the Gel-Assisted Technique where C_{en} = 0 mM

GUV	β	E_a (kV/cm)	AR	t_2 (ms)	$P(t_3)$
EF-A	1	2	2 ± 0.32 (r_{pore} = 0.8 ± 0.2 μm)	14.4 ± 3.6	16.7%
GA-A	1	2	1.55 ± 0.34 (r_{pore} = 0.6 ± 0.2 μm)	9.8 ± 3.6	9.09%
EF-B	0.03	1.5	NA (r_{pore} = 2.3 ± 1 μm)	40.2 ± 17.2	71.4%
GA-B	0.03	1.5	0.23 ± 0.08 (r_{pore} = 1 ± 0.2 μm)	17.6 ± 3.7	0

https://doi.org/10.1021/acsomega.4c06412
ACS Omega 2025, 10, 6427−6436

Table 4. Experimental Conditions and Compositions of Vesicular Solutions Used for Electrodeformation Experiments where Vesicles are Prepared by the Gel-Assisted Method, Transmembrane Potential (V_v) of Vesicles of Radius 10−20 μm is 0.75−1.5 V, 1.5−3 V, 2.25−4.5 V, and 3.0−6.0 V for E_a = 0.5, 1, 1.5, 2.0 kV/cm Respectively, and T_{EH} Is Determined to be in the Range of 0.04−0.56 ms for E_a = 0.5 − 2 kV/cm

GUV	C_{en} (mM)	Λ_{en} (mS/cm)	Λ_{sus} (mS/cm)	β	T_L	T_{MW}
GA-A	0	1.43×10^{-3}	1.48×10^{-3}	1	0.4−0.8 ms	4.8 μs
GA-C	25	2.53	2.56	1	0.23−0.46 μs	2.8 ns
GA-D	50	4.85	5.01	∼1	0.12−0.24 μs	1.4 ns
GA-E	0.3	34.6×10^{-3}	18.2×10^{-3}	2	22−44 μs	0.3 μs
GA-F	100	9.03	4.96	1.82	0.08−0.16 μs	1.1 ns
GA-G	0.3	34.6×10^{-3}	72×10^{-3}	0.48	14−28 μs	0.12 μs
GA-H	25	2.53	4.54	0.56	0.2−0.4 μs	1.8 ns

that EF vesicles have higher initial tension possibly lower edge tension, while GA vesicles appear to have lower initial tension and higher edge tension.

Effect of Concentration of Ions. The electrodeformation experiments in physiological salt solutions are relevant in the context of extrapolating results in GUVs to biological systems. However, in the present study, several difficulties were encountered in conducting systematic experiments in GUVs with a physiological (∼137 mM NaCl) salt solution. These include limitations in applying strong fields (E_a ∼ 1 kV/cm) due to very high electrohydrodynamic flows and electrolysis observed in these systems, among others. Therefore, in the electrodeformation experiments conducted in the present work, the electric field and concentration of salt in the suspending medium were carefully tuned to avoid such problems. To understand the effect of salt concentration, vesicles were prepared in low ionic ($C_{en} \leq 0.3$ mM NaCl in deionized water) as well as high ionic ($25 \leq C_{en} \leq 100$ mM NaCl) medium and were subjected to a DC pulsed electric field. Table 4 shows the vesicular samples used in these experiments, which indicate that all vesicles are fully charged at the end of the pulse. Figure 5 shows the comparison of shape deformation and degree of deformation of vesicles prepared in the low and high ionic medium for β = 1 whereas relaxation of these vesicles is depicted in Figure 6. A comparison of deformation characteristics of vesicles is shown in Figures 7 and 8 for $\beta > 1$. Deformation and relaxation characteristics of vesicles prepared in the low and high ionic medium are compared in Figures 9−13 for $\beta < 1$. Table 5 summarizes the relaxation characteristics of these vesicles at E_a = 2 kV/cm. It is to be noted that values of β in a low ionic medium and a high ionic medium were roughly the same.

For β = 1, Figure 5a,b depicts the shape deformations of vesicles at t = 1 ms for vesicles GA-A (low concentration) and vesicles GA-C (high concentration, 25 mM NaCl), respectively. The degree of deformation of these vesicles is shown in Figure 5c. Additionally, for E_a = 1 kV/cm, data for GA-D (50 mM NaCl), is also shown(Figure 5c). From Figure 5c, it is clear that the degree of deformation shows a very weak dependence on C_{en}. Moreover, vesicles GA-A and GA-C exhibit nearly similar relaxation (t_2 mechanism) characteristics (refer to Table 5 and Figure 6) at E_a = 2 kV/cm.

For $\beta > 1$, the vesicles GA-E (low concentration) and GA-F (high concentration) are subjected to an electric field in the range 0.5−2.0 kV/cm. Vesicles at low electric fields (E_a = 0.5 kV/cm) did not show any perceptible deformation. When the electric field is increased (≥1 kV/cm), prolate cylindrical deformation (refer to Figure 7a,b) is observed. Figure 7c clearly shows that the degree of deformations in both cases is

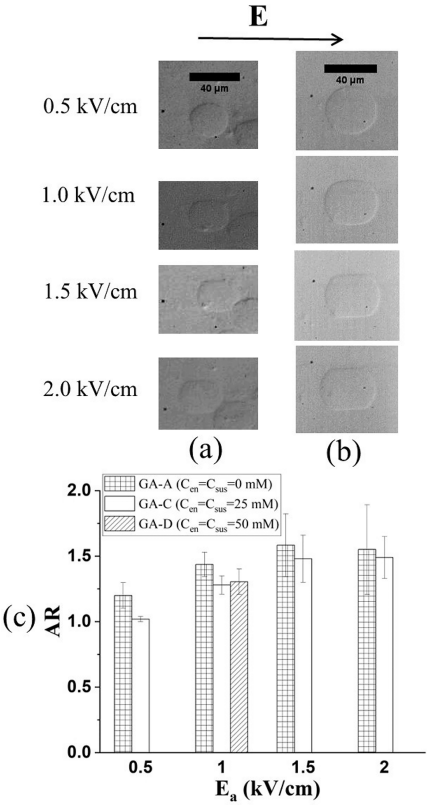

Figure 5. Microscopy images of shape deformations of vesicle (a) GA-A, and (b) GA-C, corresponding to β = 1, at t = 1 ms for E_a = 0.5−2 kV/cm, and (c) comparison of AR of vesicles at t = 1 ms.

nearly the same. However, interestingly, Figure 8 shows the comparison of relaxation characteristics of vesicles GA-E and GA-F, in which the majority of vesicles GA-E (∼83.3%) are observed to relax according to the t_2 and t_3 mechanisms. On the other hand, most GA-F vesicles, synthesized at higher salt concentrations, relax according to the t_2 mechanism. Although few GA-F vesicles (as marked by '+' and '×' in Figure 8b) might appear to relax according to both the t_2 and t_3 mechanism, the small (negligible) ΔA(∼0.007−0.02) suggests that these vesicles may be assumed to relax following the t_2 mechanism. The above observations demonstrate that the pore closure is much faster and fluid efflux is much smaller in the case of vesicles with higher C_{en}.

Lastly, for $\beta < 1$ the microscopy images of shape deformations of vesicles GA-G (low concentration) and GA-H (high concentration) at t = 1 ms are shown in Figures 9 and 10, respectively. Even though vesicles GA-G do not deform at a

https://doi.org/10.1021/acsomega.4c06412
ACS Omega 2025, 10, 6427−6436

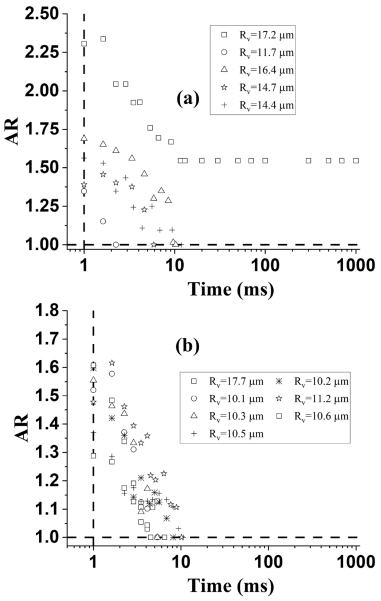

Figure 6. Relaxation of vesicles (a) GA-A and (b) GA-C where E_a = 2 kV/cm.

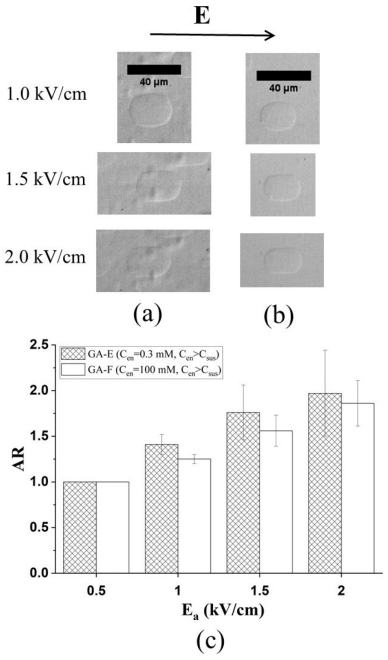

Figure 7. Microscopy images of shape deformations of vesicles (a) GA-E and (b) GA-F, corresponding to $\beta > 1$, at t = 1 ms for E_a = 0.5−2 kV/cm, and (c) comparison of AR of vesicles at t = 1 ms.

low electric field (E_a = 0.5 kV/cm), they acquire either a nearly or perfectly square shape at an electric field of 1.0 kV/cm as indicated by their AR (see Figure 11). Much pronounced oblate deformations of vesicles GA-G are observed when the electric field is increased to and beyond 1.5 kV/cm. Similar to the vesicles GA-G, vesicles GA-H do not deform while subjected to a low electric field (E_a = 0.5 kV/cm). However, contrary to the vesicles GA-G, the vesicles GA-H exhibit a significant probability of prolate deformation and squaring (Figures 10 and 12) as the electric field is increased to 1.0 kV/cm. When the electric field is further increased to 1.5 kV/cm, a co-occurrence of prolate and oblate shape deformations is

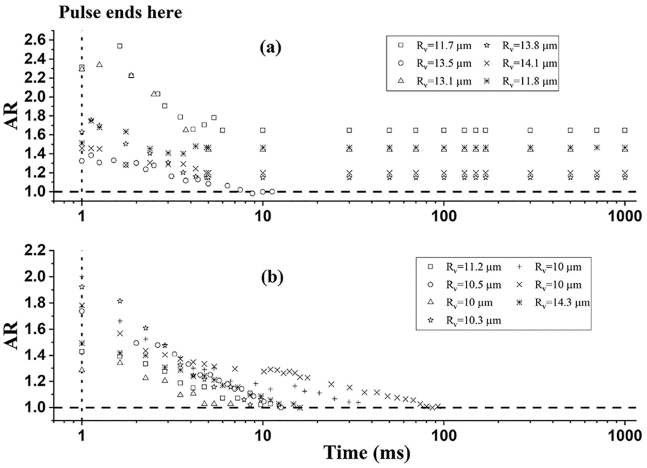

Figure 8. Relaxation of vesicles (a) GA-E and (b) GA-F where E_a = 2 kV/cm.

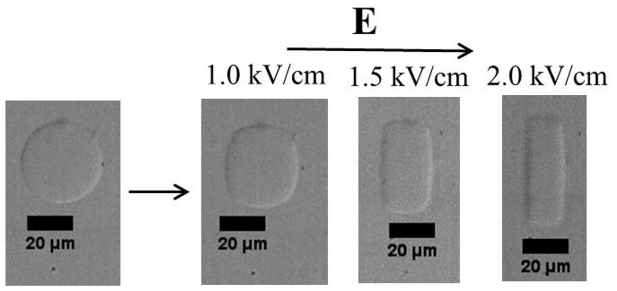

Figure 9. Microscopy images of shape deformations of vesicles GA-G at t = 1 ms, corresponding to $\beta < 1$, for E_a = 0.5−2 kV/cm.

observed. Typically, around 25% of the vesicles show oblate deformation at E_a = 1.5 kV/cm. The values of AR corresponding to prolate and oblate deformations are 1.12 ± 0.09 and 0.8 ± 0.22, respectively, for vesicles GA-H, at E_a = 1.5 kV/cm. Further increment of the electric field to 2 kV/cm leads to solely prolate deformations as indicated by their AR (AR = 1.28 ± 0.13). A closer look at Figure 10 reveals an interesting picture. At E_a = 2 kV/cm, the contrast between the inner and outer regions of the vesicle fades away, and the membrane of the vesicle becomes starkly visible. This can be due to ion transport and ionic equilibration between the inside and outside of the vesicle in the process of applying incremental electric fields, before conducting the 2 kV/cm experiment. The presence of lipid debris on the membrane was observed, which might be caused by the poration after applying an electric field of 1.5 kV/cm. It is to be noted that the dynamics of vesicles could not be captured for the intermediate time between the application of two successive electric pulses.

To ascertain the role of the incremental electric field, a few experiments were conducted by applying an electric field of 2 kV/cm directly to the vesicles GA-H. It should be noted that the contrast in these vesicles is much greater in Figure 12a1,a2 as compared to that in the third row of Figure 10a,b, indicating significant conductivity contrast. Interestingly these results (see Figure 12) show that around 23.1% of vesicles GA-H exhibit prolate deformation while being directly subjected to an electric field of 2 kV/cm instead of an incrementally increased electric field of the same strength (that is, 2 kV/cm). This suggests that in direct application of an electric field, the electroporation-induced equilibration of salt, as appears to

https://doi.org/10.1021/acsomega.4c06412
ACS Omega 2025, 10, 6427−6436

Table 5. Comparison of the Relaxation of Vesicles Prepared by the Gel-Assisted Method for Different Values of C_{en} and β for E_a = 2 kV/cm where Vesicles were Subjected to an Incremental Electric Field

GUV	C_{en} (in mM)	β	AR	t_2	$P(t_3)$
GA-A	0	1	1.55 ± 0.34	9.8 ± 3.6 ms (r_{pore} = 0.56 ± 0.21 μm)	9.1%
GA-C	25	1	1.49 ± 0.16	9 ± 2.3 ms (r_{pore} = 0.51 ± 0.13 μm)	0
GA-E	0.3	2	1.97 ± 0.47	5.8 ± 1.5 ms (r_{pore} = 0.33 ± 0.08 μm)	83.3%
GA-F	100	1.82	1.86 ± 0.25	4−100 ms (r_{pore} = 0.23−5.7 μm)	0
GA-G	0.3	0.48	0.37 ± 0.1	16.7 ± 10.1 ms (r_{pore} = 1 ± 0.6 μm)	10%
GA-H	25	0.56	1.28 ± 0.13	4.75 ± 1.2 ms (r_{pore} = 0.27 ± 0.07 μm)	0

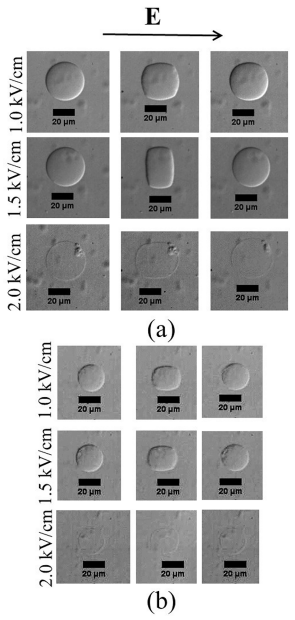

Figure 10. Microscopy images of shape deformations of vesicles GA-H at t = 1 ms, corresponding to β < 1, for E_a = 0.5−2 kV/cm for two different vesicles (images shown in subfigures (a) and (b)) under the same experimental conditions. In each subfigure (a) or (b), the images in the first column indicate vesicles at t = 0 ms, images in the second column represent the shape of deformed vesicles, and images in the third column depict the relaxed vesicles. The corresponding electric fields are mentioned in the left side of the images.

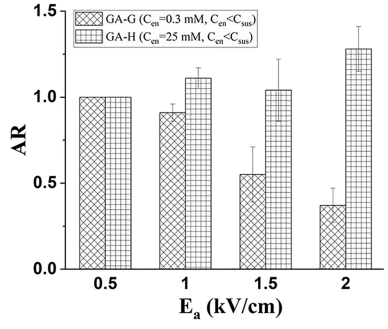

Figure 11. Comparison of AR of vesicles GA-G and GA-H at t = 1 ms, corresponding to β < 1, for E_a = 0.5−2 kV/cm.

occur for incrementally applied fields, is diminished, thereby predominantly admitting oblate deformation at 2 kV/cm.

Table 5 and Figure 13a,b show that vesicles GA-G and GA-H predominantly relaxed according to the t_2 mechanism. Vesicles GA-H relax over 4.75 ± 1.2 ms at E_a = 2 kV/cm where they underwent ionic equilibration between two successive pulses. In order to avoid confusion due to ionic equilibration, they were subjected directly to an electric field of 2 kV/cm,

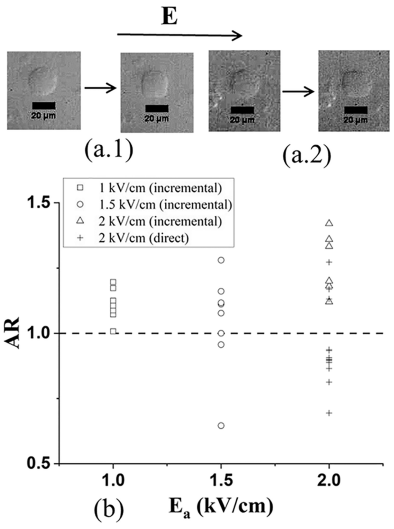

Figure 12. (a.1) and (a.2) show microscopy images of shape deformations of vesicles GA-H at t = 1 ms, corresponding to β < 1, while directly subjected to an electric field of 2 kV/cm, (b) scatter plot of the AR of vesicles GA-H, corresponding to β < 1, for E_a = 1−2 kV/cm where the phrase "incremental" implies that vesicles are subjected to incremental electrical field and the phrase "direct" refers to vesicles subjected to an electric field of single pulse.

and their relaxation characteristics (refer to Figure 13c) were noted. Interestingly, no significant change in the relaxation behavior of vesicles (t_2 = 4.45 ± 2.98 ms, $P(t_3)$ = 0) was observed. Thus the data suggest that the relaxation of vesicles GA-H vesicles is faster than that of the vesicles GA-G vesicles within the assumption of the t_2 mechanism.

CONCLUSIONS

Two important aspects relevant to electrodeformation of GUVs under strong pulsed DC electric fields are discussed in this work: similarities and differences in EF and GA methods of GUV synthesis and effect of physiologically relevant salt concentrations on electrodeformation of GUVs.

Our study of the effects of a pulsed DC electric field on giant vesicles prepared by the electroformation method and the gel-assisted method provides a new perspective. Electroformed vesicles show much greater deformation at higher electric fields than the vesicles prepared by the latter while $C_{en} \leq$ 0.3 mM.

Second, our study of the effect of salt concentration indicates that the shape deformation and degree of deformation of GUVs are unaffected even if C_{en} is increased to and beyond 25 mM for both $\Lambda_{en} = \Lambda_{sus}$ and $\Lambda_{en} > \Lambda_{sus}$. However, for $\Lambda_{en} < \Lambda_{sus}$, while oblate shapes are typically observed at low concentration ($C_{en} \leq$ 0.3 mM), microscopy images and plot of AR vs E_a show that vesicles deform into prolate shape for C_{en} = 25 mM, which can be attributed to the

https://doi.org/10.1021/acsomega.4c06412
ACS Omega 2025, 10, 6427−6436

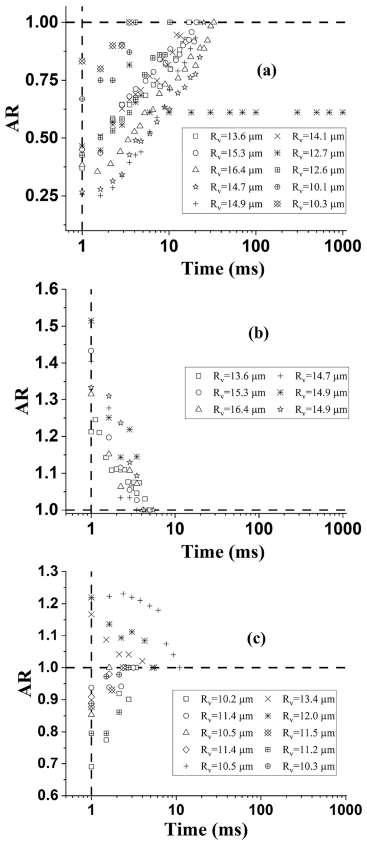

Figure 13. Relaxation of vesicles (a) GA-G and (b) GA-H while subjected to an incremental electric field for E_a = 2 kV/cm, (c) relaxation of vesicles GA-H while directly subjected to an electric field of 2 kV/cm.

ionic transport and equilibration across the bilayer membrane of GUVs.

For both $\Lambda_{en} > \Lambda_{sus}$ and $\Lambda_{en} < \Lambda_{sus}$, GUVs tend to relax faster when C_{en} is increased to 25 mM or above. This suggests a plausible mechanism where an abundance of ions increases the edge tension in the vesicles, leading to a smaller pore growth and faster pore closure. This is supported by the fact that the lipid interaction with salt is expected to be unfavorable, resulting in higher values of oil−water interfacial tension (σ_{ow}) and greater edge tension $\gamma_L = d_L\sigma_{ow}$. On the other hand, vesicles are observed to relax following the t_2 mechanism for $\Lambda_{en} = \Lambda_{sus}$ irrespective of salt concentration and the pore closure time (t_2) for both low and high salt conditions for $\Lambda_{en} = \Lambda_{sus}$ is almost of the same order. A mathematical model might help better to understand the relaxation behavior of vesicles, which is beyond the scope of the present work.

Moreover, the electroporation theory, as proposed by DeBruin and Krassowska,[43] Krassowska and Filev,[44] Smith et al.,[45] states that the conductance of a prorated membrane increases as the concentration of salt is increased. This leads to a very sharp drop in the transmembrane potential, thereby immediately suppressing further pore formation and pore growth. This seems to be another reason why pore growth is suppressed at a higher salt concentration.

It is, therefore, likely that electroporation of biological cells, which are typically at much higher salt concentration, shows much lesser membrane disruption than GUVs, which are typically investigated at low salt concentrations, at a similar order of electrical parameters, could be due to higher edge tension and faster shorting of the biomembranes at high salt concentration. The explicit role of mechanical (stiffness) properties of stiffer biological cell membranes as compared to the GUV bilayer membrane remains to be investigated.[18]

AUTHOR INFORMATION

Corresponding Author

Rochish M. Thaokar − *Department of Chemical Engineering, Indian Institute Technology of Bombay, Mumbai 400076, India;* orcid.org/0000-0003-4089-2990; Email: rochish@che.iitb.ac.in

Authors

Mohammad Maoyafikuddin − *Centre for Research in Nanotechnology & Science, Indian Institute Technology of Bombay, Mumbai 400076, India;* orcid.org/0000-0002-3860-5211

Shrikrishna V Kulkarni − *Electrical Engineering Department, Indian Institute Technology of Bombay, Mumbai 400076, India*

Complete contact information is available at: https://pubs.acs.org/10.1021/acsomega.4c06412

Notes

The authors declare no competing financial interest.

ACKNOWLEDGMENTS

We acknowledge Department of Science & Technology, New Delhi, India, for financial support.

REFERENCES

(1) *The Cell: A Molecular Approach.* Fourth Edition. ByCooper, G. M.; Hausman, R. E. ASM Press and Sunderland (Massachusetts): Sinauer Associates: Washington (DC). 2007, 43−72.

(2) Vlahovska, P. M.; Gracià, R. S.; Aranda-Espinoza, S.; Dimova, R. Electrohydrodynamic Model of Vesicle Deformation in Alternating Electric Fields. *Biophys. J.* **2009**, *96*, 4789−4803.

(3) Rems, L.; Tarek, M.; Casciola, M.; Miklavčič, D. Properties of lipid electropores II: Comparison of continuum-level modeling of pore conductance to molecular dynamics simulations. *Bioelectrochemistry* **2016**, *112*, 112−124.

(4) Fošnarič, M.; Kralj-Iglič, V.; Bohinc, K.; Iglič, A.; May, S. Stabilization of Pores in Lipid Bilayers by Anisotropic Inclusions. *The Journal of Physical Chemistry B* **2003**, *107*, 12519−12526.

(5) Kumar, R.; Chakrabarti, R.; Thaokar, R. M. Compound giant unilamellar vesicles as a bio-mimetic model for electrohydrodynamics of a nucleate cell. *Soft Matter* **2024**, *20*, 6995−7011.

(6) Perrier, D. L.; Vahid, A.; Kathavi, V.; Stam, L.; Rems, L.; Mulla, Y.; Muralidharan, A.; Koenderink, G. H.; Kreutzer, M. T.; Boukany, P. E. Response of an actin network in vesicles under electric pulses. *Sci. Rep.* **2019**, *9*, 8151.

(7) Riske, K. A.; Dimova, R. Electro-Deformation and Poration of Giant Vesicles Viewed with High Temporal Resolution. *Biophys. J.* **2005**, *88*, 1143−1155.

(8) Riske, K. A.; Dimova, R. Electric Pulses Induce Cylindrical Deformations on Giant Vesicles in Salt Solutions. *Biophys. J.* **2006**, *91*, 1778−1786.

(9) Maoyafikuddin, M.; Thaokar, R. M. Effect of the Waveform of the Pulsed Electric Field on the Cylindrical Deformation of Uncharged Giant Unilamellar Vesicles. *Langmuir* **2023**, *39*, 9660−9670.

(10) Salipante, P. F.; Vlahovska, P. M. Vesicle deformation in DC electric pulses. *Soft Matter* **2014**, *10*, 3386−3393.

(11) Tekle, E.; Astumian, R.; Friauf, W.; Chock, P. Asymmetric Pore Distribution and Loss of Membrane Lipid in Electroporated DOPC Vesicles. *Biophys. J.* **2001**, *81*, 960−968.

https://doi.org/10.1021/acsomega.4c06412
ACS Omega 2025, 10, 6427−6436

(12) Portet, T.; i Febrer, F. C.; Escoffre, J.-M.; Favard, C.; Rols, M.-P.; Dean, D. S. Visualization of Membrane Loss during the Shrinkage of Giant Vesicles under Electropulsation. *Biophys. J.* **2009**, *96*, 4109−4121.
(13) Dimova, R.; Riske, K. A.; Aranda, S.; Bezlyepkina, N.; Knorr, R. L.; Lipowsky, R. Giant vesicles in electric fields. *Soft Matter* **2007**, *3*, 817.
(14) Perrier, D. L.; Rems, L.; Boukany, P. E. Lipid vesicles in pulsed electric fields: Fundamental principles of the membrane response and its biomedical applications. *Adv. Colloid Interface Sci.* **2017**, *249*, 248−271.
(15) Ando, T.; Skolnick, J. Crowding and hydrodynamic interactions likely dominate in vivo macromolecular motion. *Proceedings of the National Academy of Sciences* **2010**, *107*, 18457−18462.
(16) Leontiadou, H.; Mark, A. E.; Marrink, S.-J. Ion Transport across Transmembrane Pores. *Biophys. J.* **2007**, *92*, 4209−4215.
(17) Mou, Q.; Xu, M.; Deng, J.; Hu, N.; Yang, J. Studying the roles of salt ions in the pore initiation and closure stages in the biomembrane electroporation. *APL Bioeng.* **2023**, *7*, No. 026103.
(18) Sabri, E.; Aleksanyan, M.; Brosseau, C.; Dimova, R. Effects of solution conductivity on macropore size dynamics in electroporated lipid vesicle membranes. *Bioelectrochemistry* **2022**, *147*, No. 108222.
(19) Angelova, M. I.; Dimitrov, D. S. Liposome electroformation. *Faraday Discuss. Chem. Soc.* **1986**, *81*, 303.
(20) Zhou, Y.; Berry, C. K.; Storer, P. A.; Raphael, R. M. Peroxidation of polyunsaturated phosphatidyl-choline lipids during electroformation. *Biomaterials* **2007**, *28*, 1298−1306.
(21) Dimova, R.; Aranda, S.; Bezlyepkina, N.; Nikolov, V.; Riske, K. A.; Lipowsky, R. A practical guide to giant vesicles. Probing the membrane nanoregime via optical microscopy. *Journal of Physics: Condensed Matter* **2006**, *18*, S1151−S1176.
(22) Makky, A.; Tanaka, M. Impact of Lipid Oxidization on Biophysical Properties of Model Cell Membranes. *The Journal of Physical Chemistry B* **2015**, *119*, 5857−5863.
(23) Horger, K. S.; Estes, D. J.; Capone, R.; Mayer, M. Films of Agarose Enable Rapid Formation of Giant Liposomes in Solutions of Physiologic Ionic Strength. *J. Am. Chem. Soc.* **2009**, *131*, 1810−1819.
(24) Weinberger, A.; Tsai, F.-C.; Koenderink, G. H.; Schmidt, T. F.; Itri, R.; Meier, W.; Schmatko, T.; Schröder, A.; Marques, C. Gel-Assisted Formation of Giant Unilamellar Vesicles. *Biophys. J.* **2013**, *105*, 154−164.
(25) Faizi, H. A.; Tsui, A.; Dimova, R.; Vlahovska, P. M. Bending Rigidity, Capacitance, and Shear Viscosity of Giant Vesicle Membranes Prepared by Spontaneous Swelling, Electroformation, Gel-Assisted, and Phase Transfer Methods: A Comparative Study. *Langmuir* **2022**, *38*, 10548−10557.
(26) Estes, D. J.; Mayer, M. Electroformation of giant liposomes from spin-coated films of lipids. *Colloids and Surfaces B: Biointerfaces* **2005**, *42*, 115−123.
(27) Maoyafikuddin, M.; Pundir, M.; Thaokar, R. Starch aided synthesis of giant unilamellar vesicles. *Chemistry and Physics of Lipids* **2020**, *226*, No. 104834.
(28) Kinosita, K.; Ashikawa, I.; Saita, N.; Yoshimura, H.; Itoh, H.; Nagayama, K.; Ikegami, A. Electroporation of cell membrane visualized under a pulsed-laser fluorescence microscope. *Biophys. J.* **1988**, *53*, 1015−1019.
(29) Jones, T. B. *Electromechanics of Particles*; Cambridge University Press, 1995.
(30) Taylor, G. I. Studies in electrohydrodynamics. I. The circulation produced in a drop by an electric field. *Proc. R. Soc. Lond. Ser. A Math. Phys. Sci.* **1966**, *291*, 159−166.
(31) Grosse, C.; Zimmerman, V. Numerical Calculation of the Dielectric and Electrokinetic Properties of Vesicle Suspensions. *The Journal of Physical Chemistry B* **2005**, *109*, 18088−18095.
(32) Needham, D.; Hochmuth, R. Electro-mechanical permeabilization of lipid vesicles. Role of membrane tension and compressibility. *Biophys. J.* **1989**, *55*, 1001−1009.
(33) Ardham, V. R.; Zoni, V.; Adamowicz, S.; Campomanes, P.; Vanni, S. Accurate Estimation of Membrane Capacitance from Atomistic Molecular Dynamics Simulations of Zwitterionic Lipid Bilayers. *The Journal of Physical Chemistry B* **2020**, *124*, 8278−8286.
(34) Das, S.; Tian, A.; Baumgart, T. Mechanical Stability of Micropipet-Aspirated Giant Vesicles with Fluid Phase Coexistence. *The Journal of Physical Chemistry B* **2008**, *112*, 11625−11630.
(35) Song, J.; Waugh, R. Bending rigidity of SOPC membranes containing cholesterol. *Biophys. J.* **1993**, *64*, 1967−1970.
(36) James, H. P.; Jadhav, S. Mechanical and transport properties of chitosan-zwitterionic phospholipid vesicles. *Colloids and Surfaces B: Biointerfaces* **2020**, *188*, No. 110782.
(37) Evans, E.; Rawicz, W. Entropy-driven tension and bending elasticity in condensed-fluid membranes. *Phys. Rev. Lett.* **1990**, *64*, 2094−2097.
(38) Schneider, M.; Jenkins, J.; Webb, W. Thermal fluctuations of large cylindrical phospholipid vesicles. *Biophys. J.* **1984**, *45*, 891−899.
(39) Althoff, G.; Stauch, O.; Vilfan, M.; Frezzato, D.; Moro, G. J.; Hauser, P.; Schubert, R.; Kothe, G. Transverse Nuclear Spin Relaxation Studies of Viscoelastic Properties of Membrane Vesicles. II. Experimental Results. *The Journal of Physical Chemistry B* **2002**, *106*, 5517−5526.
(40) Brochard-Wyart, F.; de Gennes, P.; Sandre, O. Transient pores in stretched vesicles: role of leak-out. *Physica A: Statistical Mechanics and its Applications* **2000**, *278*, 32−51.
(41) Teissie, J. In *Handbook of Electroporation*; Miklavčič, D., Ed.; Springer International Publishing: Cham, 2017; 25−43.
(42) Das, S.; Jaeger, M.; Leonetti, M.; Thaokar, R. M.; Chen, P. G. Effect of pulse width on the dynamics of a deflated vesicle in unipolar and bipolar pulsed electric fields. *Phys. Fluids* **2021**, *33*, No. 081905.
(43) DeBruin, K. A.; Krassowska, W. Modeling Electroporation in a Single Cell. II. Effects of Ionic Concentrations. *Biophys. J.* **1999**, *77*, 1225−1233.
(44) Krassowska, W.; Filev, P. D. Modeling Electroporation in a Single Cell. *Biophys. J.* **2007**, *92*, 404−417.
(45) Smith, K. C.; Neu, J. C.; Krassowska, W. Model of Creation and Evolution of Stable Electropores for DNA Delivery. *Biophys. J.* **2004**, *86*, 2813−2826.

https://doi.org/10.1021/acsomega.4c06412
ACS Omega 2025, 10, 6427−6436